

Single-particle spectral weight of a two-dimensional Hubbard model

E. Dagotto and F. Ortolani*

Department of Physics and Center for Materials Research and Technology, Florida State University, Tallahassee, Florida 32306

D. Scalapino

Department of Physics and Institute for Theoretical Physics, University of California at Santa Barbara, Santa Barbara, California 93106

(Received 12 February 1992)

Numerical results for the single-particle spectral weight $A(\mathbf{p}, \omega)$ and the density of states $N(\omega)$ for a 4×4 Hubbard model are presented. Both the half filled insulating state and the doped metallic state are considered. At half filling the numerical results are compared with the mean-field spin-density-wave single-particle spectral weight, and away from half filling with a renormalized quasiparticle band description. The relationship of these results to experimental photoemission, inverse photoemission, and angular-resolved measurements is discussed.

Information on the single-particle energy density of states $N(\omega)$ can be obtained from photoemission (PES) and inverse photoemission spectroscopy (IPES) which produce final states with one extra hole or electron, via photon absorption and electron emission, or electron injection and photon emission, respectively.^{1,2} Recently, results from angular-resolved photoemission spectroscopy

(ARPES) on c -axis-normal oriented single crystals of various high- T_c oxide superconductors have been reported.³ Using the sudden approximation to describe the photon process, the angular-resolved PES and IPES scattering rates are proportional to the single-particle spectral weight $A(\mathbf{p}, \omega)$. At zero temperature,

$$A(\mathbf{p}, \omega) = \begin{cases} \sum_n |{}_{N+1}\langle n | c_{\mathbf{p},s}^\dagger | 0 \rangle_N|^2 \delta(\omega - (E_n^{N+1} - E_0^N)), & \omega > \mu, \\ \sum_n |{}_{N-1}\langle n | c_{\mathbf{p},s} | 0 \rangle_N|^2 \delta(\omega + (E_n^{N-1} - E_0^N)), & \omega < \mu. \end{cases} \quad (1)$$

μ is the chemical potential and the rest of the notation is standard.⁴ For $\omega > \mu$, $A(\mathbf{p}, \omega)$ describes the ARPES process, while for $\omega < \mu$, $A(\mathbf{p}, \omega)$ with energy equal to $|\omega - \mu|$ determines the IPES. If events over a sufficiently large angle are accepted, then PES and IPES provide information on the energy density of states $N(\omega) \sim \sum_{\mathbf{p}} A(\mathbf{p}, \omega)$, for $\omega < \mu$ and $\omega > \mu$, respectively.

In order to gain insight into the nature of the single-particle spectral weight for a strongly correlated electron system, we have carried out Lanczos calculations of $A(\mathbf{p}, \omega)$ and $N(\omega)$ for two-dimensional (2D) Hubbard clusters. Results for a $\sqrt{10} \times \sqrt{10}$ lattice have previously been reported.⁴ Here we discuss Lanczos results for a 4×4 cluster.⁵ Studying this cluster size requires a major computational effort since at half filling, the largest subspace we have studied contains $\sim 1\,350\,000$ states even after exploiting all the symmetries of the model.⁶ Lanczos results for ground-state energies and the optical conductivity, $\sigma(\omega)$, have been previously presented for this cluster.^{6,7} Based upon Monte Carlo results⁸ and 4×4 and 8×8 lattices for various susceptibilities, we believe that the 4×4 lattice is sufficiently large that it can provide useful insight into the physical properties of the 2D Hubbard model, particularly when U is greater than or of the order of the bandwidth $8t$. Here we present these results, comparing them with mean-field theory for the half filled insu-

lating case and quasiparticle band theory results for the doped metallic case. We conclude by discussing the apparent conflict between our results and experiments with some suggestions for further comparison.

The spectral weights we will discuss are for a two-dimensional Hubbard model with a near-neighbor hopping t and an on-site Coulomb interaction U ,

$$H = -t \sum_{\langle ij \rangle, s} (c_{i,s}^\dagger c_{j,s} + c_{j,s}^\dagger c_{i,s}) + U \sum_i (n_{i\uparrow} - \frac{1}{2})(n_{i\downarrow} - \frac{1}{2}). \quad (2)$$

The notation is standard and we have written the interaction in a form such that the chemical potential is zero for a half filled band. Here we will focus on results obtained for U equal to the bandwidth $8t$ and various fillings, although we have also performed calculations for $U=4, 10$, and 20 . Monte Carlo simulations combined with a finite-size scaling analysis on lattices up to 12×12 have shown that the half filled, $\langle n_{i\uparrow} + n_{i\downarrow} \rangle = \langle n \rangle = 1$, ground state has long-range antiferromagnetic order.^{8,9} Drude weight calculations imply that the ground state is insulating as expected.⁷ In this case we have found that a mean-field, spin-density-wave approximation provides a sensible starting point for understanding the momentum distribution $\langle n_{\mathbf{p}} \rangle$ as well as various other properties.⁸ Using this same approximation, we obtain a spectral weight

$$A(\mathbf{p}, \omega)_{\text{MF}} = \frac{1}{2} (1 + \epsilon_{\mathbf{p}}/E_{\mathbf{p}}) \delta(\omega - E_{\mathbf{p}}) + \frac{1}{2} (1 - \epsilon_{\mathbf{p}}/E_{\mathbf{p}}) \delta(\omega + E_{\mathbf{p}}), \quad (3)$$

with $E_{\mathbf{p}} = (\epsilon_{\mathbf{p}}^2 + \Delta_{\text{SDW}}^2)^{1/2}$ and $\epsilon_{\mathbf{p}} = -2t(\cos p_x + \cos p_y)$. Here Δ_{SDW} is the spin-density-wave gap, given in mean-field theory by the solution of

$$1 = \frac{U}{N} \sum_{\mathbf{p}} \frac{\tanh(\beta E_{\mathbf{p}}/2)}{2E_{\mathbf{p}}}. \quad (4)$$

Broadening the delta functions in Eq. (3) by $0.2t$, we obtain the mean-field spectral weights shown for various momentum values in Fig. 1. Here we have replaced U in Eq. (4) by a reduced value $\bar{U} \sim 5.2$ chosen to give the same Δ_{SDW} gap obtained in the Lanczos calculations which follow.¹⁰ We have also used a reduced value for $t^* = 0.65$ in $\epsilon_{\mathbf{p}} = -2t^*(\cos p_x + \cos p_y)$ obtained from Monte Carlo data.⁸ For $\mathbf{p} = (\pi, 0)$ or any other momentum on the noninteracting half filled Fermi surface, where $\epsilon_{\mathbf{p}}$ vanishes, the broadened mean-field form, Eq. (3), consists of two equal contributions, as shown in Fig. 1(a). Note that the chemical potential for half filling, $\langle n \rangle = 1$, is zero. As \mathbf{p} decreases to $(\pi/2, 0)$, the spectral weight shifts to the PES, negative ω regime, see Fig. 1(b). This behavior continues, as shown in Fig. 1(c), for $\mathbf{p} = (0, 0)$, where over 87% of the spectral weight lays in the PES, $\omega < 0$, part of the spectrum. As is well known, the area under $A(\mathbf{p}, \omega)$ is unity so that as the PES weight increases, the IPES weight must decrease. This system is particle-hole symmetric so that when \mathbf{p} goes outside the noninteracting Fermi surface, the spectral weight shifts towards the IPES, $\omega > 0$, regime. For example, the $\mathbf{p} = (\pi, \pi)$ spectral weight is obtained by reflecting Fig. 1(c) about the origin. Finally, in Fig. 1(d) we show the density of states $N(\omega)$ in the mean-field approximation obtained with a cluster large enough such that finite-size effects are negligible.

In Figs. 2(a)–2(c) we show the spectral weight ob-

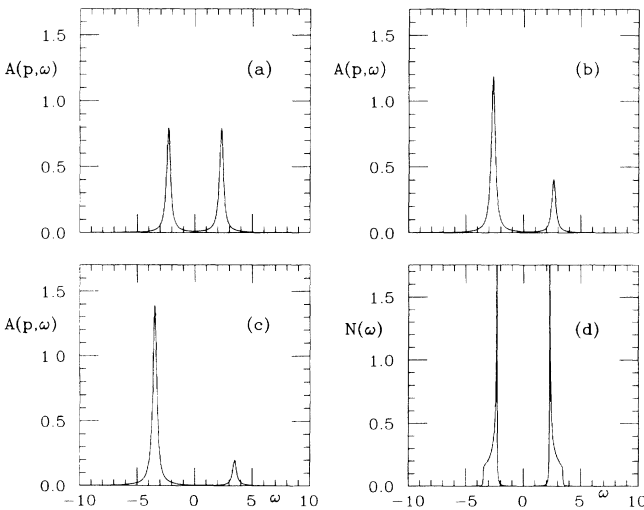


FIG. 1. Mean-field spectral weight $A(\mathbf{p}, \omega)$ vs ω in units where $t = 1$ for (a) $\mathbf{p} = (\pi, 0)$, (b) $\mathbf{p} = (\pi/2, 0)$, and (c) $\mathbf{p} = (0, 0)$. (d) The mean-field density of states for a 125×125 cluster. At half filling the chemical potential is zero.

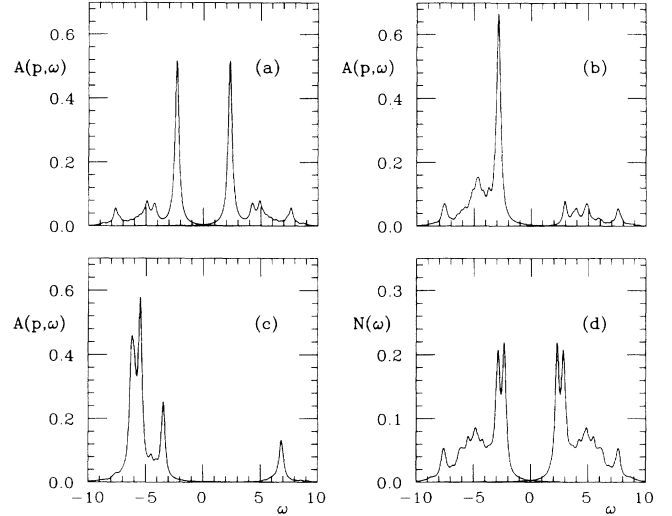


FIG. 2. Lanczos calculations of the spectral weights for a half filled, $\langle n \rangle = 1$, 4×4 lattice with $U = 8t$. The momenta are the same as in Fig. 1, i.e., (a) $\mathbf{p} = (\pi, 0)$, (b) $\mathbf{p} = (\pi/2, 0)$, and (c) $\mathbf{p} = (0, 0)$. (d) The single-particle density of states, $N(\omega)$, vs ω .

tained from a Lanczos calculation for a half filled 4×4 lattice with $U = 8t$ at the same momenta as the mean-field results of Fig. 1. In this case a broadening of $0.2t$ was also used in plotting the Lanczos results. Here at half filling and $\mathbf{p} = (\pi, 0)$, there are clearly two quasiparticle peaks split by $2\Delta_{\text{SDW}} = 4.6t$.¹¹ The exchange energy J is of order $4t^2/U = 0.5t$ so that the shakeoff of spin fluctuations¹² provides structure and damping on this fluctuation, while the band structure of width $8t$ and the Coulomb interaction $U = 8t$ provide the large-scale energy structure. At $\mathbf{p} = (\pi/2, 0)$, the quasiparticle weight has shifted deeper into the PES, $\omega < 0$ region, and only a small remnant structure remains visible at $\omega \sim 3t$ on the IPES side. The quasiparticle peak position at $\mathbf{p} = (\pi/2, 0)$ is in good agreement with the mean-field result shown in Fig. 2(b). For $\mathbf{p} = (0, 0)$, Fig. 2(c), the spectral weight has shifted to still higher energies and the notion of a well-defined quasiparticle is questionable. Note the presence of large spectral weight at $\omega \sim -6t$. Summing over all momenta, we obtain the density of states $N(\omega)$ shown in Fig. 2(d). Here the Mott-Hubbard gap is clearly visible.

Turning next to the doped case, Figs. 3(a)–3(f) show results for the spectral weight for $\langle n \rangle = 0.875$, $U/t = 8$, and $\Gamma = 0.2t$.¹³ In these figures, the chemical potential is located at $\mu = -2.4t$ (see Ref. 4). The PES spectrum is associated with the spectral weight below μ and the IPES is associated with the weight above μ . Note that $\mathbf{p} = (\pi, 0)$ lays outside the noninteracting Fermi surface and the dominant spectral weight lays in the IPES region. Here we see a well-defined quasiparticle peak located near the top of the lower Hubbard band of the half filled insulating case previously discussed (Fig. 2). Remnants of the upper Hubbard band are also clearly visible. It appears that the effect of hole doping is to remove spectral weight from both the upper and lower Hubbard bands and create new states in the gap at the upper edge of what was in the undoped system, the lower Hubbard band.

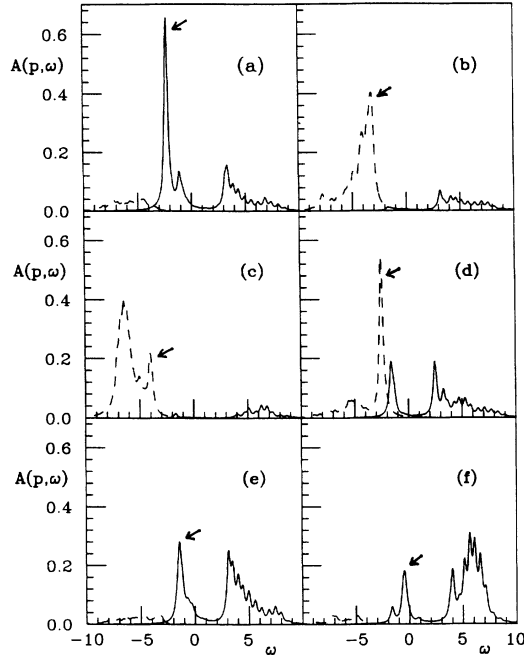


FIG. 3. Spectral weights $A(\mathbf{p}, \omega)$ for the 4×4 lattice with $U=8t$ and $\langle n \rangle=0.875$. Here the chemical potential is at $\mu = -2.4$. The IPES weight is drawn as a solid curve and the PES weight is dashed. The momentum values are (a) $\mathbf{p}=(\pi, 0)$, (b) $\mathbf{p}=(\pi/2, 0)$, and (c) $\mathbf{p}=(0, 0)$ just as in Figs. 1 and 2. Here, however, in the doped case, the particle-hole symmetry is broken so that we also show the spectral weight at (d) $\mathbf{p}=(\pi/2, \pi/2)$, (e) $\mathbf{p}=(\pi, \pi/2)$, and (f) $\mathbf{p}=(\pi, \pi)$. The arrows mark the peaks used to obtain the “quasiparticle” dispersion plotted in Fig. 4(a).

At $\mathbf{p}=(\pi/2, 0)$, one is inside the noninteracting Fermi surface and we see that the weight has shifted to the PES as expected. Here the quasiparticle peak is significantly broader than the corresponding structure for the half filled case Fig. 2(b). At $\mathbf{p}=(0, 0)$, the spectral weight behaves similarly to the undoped case with most of the spectral weight concentrated at high energies. The point nearest to the noninteracting Fermi surface is $\mathbf{p}=(\pi/2, \pi/2)$. Here in Fig. 3(d), we see a well-defined quasiparticle peak in the PES and a small peak in the IPES just above the chemical potential. Figures 3(a) and 3(d) imply an interacting Fermi surface as shown in the inset in Fig. 4(a), i.e., one where $\mathbf{p}=(0, \pi)$ is empty but $\mathbf{p}=(\pi/2, \pi/2)$ is at least partially occupied.¹⁴ In Figs. 3(e) and 3(f), corresponding to $\mathbf{p}=(\pi, \pi/2)$ and $\mathbf{p}=(\pi, \pi)$, respectively, we see again clear evidence for weight split off from the upper and lower Hubbard bands to produce states in the gap of the $\langle n \rangle=1$ insulator near the top of the lower Hubbard band. The presence of these new states form a pseudogap. For the larger values of the Coulomb repulsion, the gap is not filled upon doping, while for smaller couplings, the upper and lower Hubbard bands merge and little trace of the original gap is left.

In Fig. 4(a) we have plotted the dispersion of the peaks denoted by arrows in Fig. 3. The resulting dispersion relation is similar to the simple band structure $\epsilon_{\mathbf{p}} = -2t^*(\cos p_x + \cos p_y)$ with a reduced $t^*=0.7$. Clearly,

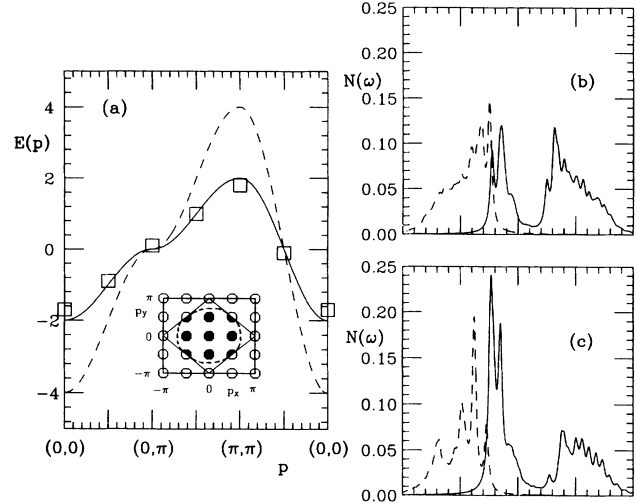


FIG. 4. (a) Energy of the quasiparticle as a function of momentum (\square). The solid line shows the quasiparticle band structure $\epsilon_{\mathbf{p}} = -2t^*(\cos p_x + \cos p_y)$ with $t^*=0.70$, while the dashed line is the noninteracting dispersion relation ($t^*=t=1$). The points are obtained from the peaks in the spectral weight denoted by the arrows in Fig. 3. The inset is a schematic illustration of the ground-state occupation of the interacting 4×4 lattice with $\langle n \rangle=0.875$ and $U=8$. The dashed line in the inset represents the Fermi surface. (b) The single-particle density of states $N(\omega)$ vs ω for the 4×4 lattice with $U=8t$ and $\langle n \rangle=0.875$. (c) Same as (b) but for $\langle n \rangle=0.75$.

the small number of \mathbf{p} points makes this at best a qualitative comparison. Summing over all momenta gives the density of states $N(\omega)$ for $\langle n \rangle=0.875$ shown in Fig. 4(b). Comparing this with the $\langle n \rangle=1$ case shown in Fig. 2(d), one clearly sees that the effect of hole doping is to remove spectral weight at the upper and lower Hubbard bands of the insulator and create a new spectral weight at the upper edge of the lower Hubbard band. The results for $N(\omega)$ with additional doping, $\langle n \rangle=0.75$ are shown in Fig. 4(c). As can be seen, additional weight is pulled into the gap of the $\langle n \rangle=1$ insulator and μ has decreased further. This trend continues at higher dopings.

In conclusion, the similarity of these 4×4 results with earlier $\sqrt{10} \times \sqrt{10}$ results⁴ leads us to believe that the basic structure of the single-particle spectral weight discussed above is characteristic of the one-band Hubbard model. At smaller values of the Coulomb interaction, for example $U=4t$, the gap is less clearly defined and upon doping new states fill the entire gap. Nevertheless, μ is still found to shift across a significant portion of the insulating gap when the doping is changed from holes to electrons. Furthermore, in all cases, spectral weight is removed from both the upper and lower bands of the insulator and distributed into the gaps with more weight near the top of the lower band for hole doping and near the bottom of the upper band for electron doping. In addition, $A(\mathbf{p}, \omega)$ in both the insulating and metallic state has peaks which exhibit dispersive, quasiparticle bandlike characteristics. In the insulating state, the quasiparticle dispersion varies as $(\epsilon_{\mathbf{p}}^2 + \Delta_{\text{SDW}}^2)^{1/2}$, with peaks in both the PES and IPES spectra. In the metallic state, a renormalized band struc-

ture $\epsilon_p = -2t^*(\cos p_x + \cos p_y)$ provided a reasonable fit to the dispersion of a particular peak in $A(\mathbf{p}, \omega)$. Due to the coarse momentum grid associated with a 4×4 lattice we are unable to obtain information on the effective mass.

Certain features of these results are in apparent disagreement with PES and IPES experiments. In particular, work of $\text{La}_{2-x}\text{Sr}_x\text{CuO}_{4+\delta}$ indicates that the chemical potential μ does not appear to move as the doping increases.² Rather than new states appearing at the top of the valence band of the insulator, hole doping appears to create states near the center of the gap. Furthermore, in $\text{Nd}_{2-x}\text{Ce}_x\text{CuO}_{4-\delta}$, PES data¹ have been interpreted as showing that μ does not move across the gap to new states formed at the bottom of the conduction band of the insulator but rather that μ has roughly the same position relative to the valence-band maximum as in $\text{La}_{2-x}\text{Sr}_x\text{CuO}_{4+\delta}$. This disagreement makes it difficult to know how one should compare the other spectral features. As we have seen, the Lanczos results show dispersive features for both the insulating and metallic cases. In addition, our numerical results clearly illustrate the failure of a rigid band picture. These general features are also seen experimentally; however, the problem of the position of the chemical potential and the apparent similarity of the electron and hole doped spectral weights remains puzzling. It should be noted that other techniques for probing the spectral weight such as x-ray absorption¹⁵ in which an electron is excited from a core level to an unoccupied state, appear to be in reasonable agreement with the be-

havior of the spectral weight we have found. As noted by Allen *et al.*,¹ such x-ray absorption spectroscopy (XAS) techniques have the disadvantage that they are not as simply related to $A(\mathbf{p}, \omega)$ as the PES and IPES techniques. However, XAS does probe the bulk rather than the surface layers.

We believe that it would be interesting to examine the ARPES of the insulating state (if possible) and look for dispersive states which follow $(\epsilon_p^2 + \Delta_{SDW}^2)^{1/2}$. Here one could also look for the weaker, $(1 - \epsilon_p/E_p)$ [see Eq. (3)], quasiparticle feature when $\mathbf{p} > \mathbf{p}_F$. This type of study would not only provide a further area of comparison with theory but could also provide an indication of what could be expected if an outerlayer of the doped material becomes insulating. In addition, we believe that it is important to determine whether the Madelung potential can shift the effective chemical potential of the surface layers. If the present disagreement between experiments and the results we have presented remain, one will need to look beyond the one-band Hubbard model.

We thank J. W. Allen, E. Manousakis, A. Moreo, F. Parmigiani, J. R. Schrieffer, J. Torrance, and Z.-X. Shen for useful discussions. This work was partially supported by NSF under Grants No. PHY89-04035 and No. DMR90-02492, and the Electric Power Research Institute. The computer calculations were done at the Cray-2, NCSA, Urbana, IL.

*Permanent address: Dipartimento di Fisica, Istituto Nazionale di Fisica Nucleare, Universit'a di Bologna, via Irnerio 46, I-40126 Bologna, Italy.

¹J. W. Allen *et al.*, in Proceedings of the Adriatico Conference on Open Problems in Strongly Interacting Electron Systems [Int. J. Mod. Phys. B (to be published)]; J. W. Allen *et al.*, Phys. Rev. Lett. **64**, 595 (1990); T. Watanabe *et al.*, Phys. Rev. B **44**, 5316 (1991).

²Z.-X. Shen *et al.*, Phys. Rev. B **36**, 8414 (1987).

³R. List *et al.*, Phys. Rev. B **38**, 11966 (1988); A. Arko *et al.*, *ibid.* **40**, 2268 (1989); C. Olson *et al.*, *ibid.* **42**, 381 (1990); J. Campuzano *et al.*, Phys. Rev. Lett. **64**, 2308 (1990); T. Takahashi *et al.*, Phys. Rev. B **39**, 6636 (1989).

⁴E. Dagotto, A. Moreo, F. Ortolani, J. Riera, and D. Scalapino, Phys. Rev. Lett. **67**, 1918 (1991).

⁵Analytic continuation procedures have been used to calculate $A(\mathbf{p}, \omega)$ for the one- and three-band Hubbard models [see S. White (unpublished); G. Dopf *et al.* (unpublished)]. However, these numerical analytic continuations are not trivial. We were recently informed that Lanczos results for $N(\omega)$ on a 4×4 cluster have been independently obtained by P. W. Leung, Z. Liu, E. Manousakis, M. A. Novotny, and P. E. Openheimer (unpublished).

⁶G. Fano, F. Ortolani, and F. Seneria, Int. J. Mod. Phys. B **3**, 1845 (1989); G. Fano, F. Ortolani, and A. Parola, Phys. Rev. B **42**, 6877 (1990).

⁷E. Dagotto *et al.*, Phys. Rev. B **45**, 10107 (1992); **45**, 10741 (1992).

⁸S. R. White *et al.*, Phys. Rev. B **40**, 506 (1989); A. Moreo *et al.*, *ibid.* **41**, 2313 (1990).

⁹J. Hirsch and S. Tang, Phys. Rev. Lett. **62**, 591 (1989).

¹⁰A similar behavior has been observed in comparisons of the Monte Carlo results with random-phase approximation calculations in the paramagnetic case [N. Bulut *et al.* (unpublished)].

¹¹ $A(\mathbf{p}, \omega)$ for $\mathbf{p} = (\pi/2, \pi/2)$ and $\mathbf{p} = (\pi, 0)$ are equal on the 4×4 cluster at half filling. For the case of two holes, they are no longer identical, and thus it is difficult to predict a general rule.

¹²In the language of the t - J model, these excitations were shown to be produced by the "string" states, i.e., holes in a spin-density-wave background moving in an effective linear potential. See E. Dagotto *et al.*, Phys. Rev. B **41**, 9049 (1990), where results for $A(\mathbf{p}, \omega)$ in this model were also reported. See also M. Boninsegni and E. Manousakis, Phys. Rev. B **43**, 10353 (1991); W. Stephan and P. Horsch, Phys. Rev. Lett. **66**, 2258 (1991); Y. Hasegawa and D. Poilblanc, Phys. Rev. B **40**, 9035 (1989).

¹³The ground state of the 4×4 cluster with two holes has an accidental degeneracy between momentum $\mathbf{p} = (0, 0)$, $\mathbf{p} = (\pi, 0)$, and $\mathbf{p} = (0, \pi)$. We consider the finite momentum states unphysical, and thus our results in Figs. 3 and 4 are obtained using the $\mathbf{p} = (0, 0)$ (d wave) as the unique ground state. Certainly the results would be different using the other possible ground states.

¹⁴Similar results were obtained in the context of the t - J model by D. Poilblanc and E. Dagotto, Phys. Rev. B **42**, 4861 (1990).

¹⁵C. T. Chen, *et al.*, Phys. Rev. Lett. **66**, 104 (1991); H. Romberg *et al.*, Phys. Rev. B **42**, 8768 (1990); M. S. Hybertsen, E. Stechel, W. Foulkes, and M. Schlütter (unpublished).